Initial- and final-state excitations in $KL_{23}L_{23}$ Auger spectra of Cu and Ni metals, induced near threshold

L. Kövér,[1] Z. Berényi,[1] I. Cserny,[1] L. Lugosi,[1,4] W. Drube,[2] T. Mukoyama,[3] and V. R. R. Medicherla[2]
[1]*Institute of Nuclear Research of the Hungarian Academy of Sciences, P.O. Box 51, H-4032 Debrecen, Hungary*
[2]*Hamburger Synchrotronstrahlungslabor HASYLAB at Deutsches Elektronen-Synchrotron DESY, Notkestraβe 85, D-22603 Hamburg, Germany*
[3]*Kansai Gaidai University, Hirakata, Osaka 573-1001, Japan*
[4]*Graduate School of Materials Science, Nara Institute of Science and Technology, Surface and Materials Science Laboratory, 8916-5, Takayama, Ikoma 630-0192, Japan*
(Received 15 September 2005; revised manuscript received 20 January 2006; published 1 May 2006)

High-energy resolution $KL_{23}L_{23}$ Auger spectra of polycrystalline Cu and Ni metals were measured while tuning the energy of the exciting x-rays in the near threshold region up to 50 eV above the *K* absorption edge. The intensity evolution of the pronounced satellite lines as a function of photon energy reveals different behavior for particular satellites as a consequence of initial state and final state shake excitations. The satellite intensity development near threshold is compared to predictions of different simple models based on the free atom approximation. The observed energy separations between the satellites and the $^1D_2$ main diagram line is in accord with results from a cluster molecular orbital model and confirms the assignment based on the satellite intensity evolution curves concerning the origin of the satellites.

DOI: 10.1103/PhysRevB.73.195101 PACS number(s): 79.60.Bm, 32.80.Hd, 71.15.Qe

I. INTRODUCTION

Photon-induced *KLL* Auger spectra of solid 3*d* metals, such as Cu and Ni, contain pronounced satellites[1] as a result of excitation processes associated with the inner-shell hole creation. The spectra depend strongly on the local density of the unoccupied electronic states around the excited atom.[2] The evolution of the intensity and the peak shape of the satellites as the energy of the exciting photons is varied close to the inner-shell ionization threshold provides insight into their origin and nature. From such information, it is possible to determine whether the satellites are due to processes that are intrinsic to the photoexcitation, such as atomiclike, localized excitations, or to those that are extrinsic, such as inelastic electron scattering. In addition, it is possible to determine whether the intrinsic satellites arise from initial-state or final-state effects.[3–7] In spite of the interesting and unique information on the electronic structure of the materials that can be obtained from such data, only few studies are available so far which deal with the mechanisms of the creation of satellite peaks accompanying purely inner-shell transitions in solids.[7] The 3*d* transition metals, their alloys, and compounds are especially interesting in this respect due to the strong effects of electron correlation on the particular transitions. The $L_{2,3}VV$ satellite structure of some 3*d* metals and their alloys has been studied[3–6] and controversially discussed regarding the significance of Coster–Kronig (CK) transitions for their origin and spectral weight. All final holes in these transitions reside in the valence shell and the energy separation of the *L* edges is small which makes it difficult if not impossible to derive unambiguous conclusions from the excitation energy dependence of the satellite structure. A much clearer case is at hand with the *KLL* Auger transitions since only inner shells are involved and CK channels are absent. However, for these energetic transitions, experimental data are scarce[1,2] and experiments utilizing resonant excitation have not been reported so far. In general, a better understanding and clarification of the excitation mechanisms of the satellites is achieved by observing their behavior at near-threshold photoexcitation. In the case of *KLL* Auger spectra of Cu and Ni, the earlier identification of the origin of the satellites in the spectra was based on the measurement and calculation of energy separations only.[1,2] In some cases, on the basis of the magnitude of the energy separation, it is not clear that the origin of the satellite is due to final state excitation or to a two-electron excitation in the initial state. Therefore, the additional information from the satellite intensity evolution at near-threshold photoexcitation can be decisive. The observed intensity behavior cannot only confirm the nature of the excitation mechanism, but also provide a possibility to check the validity of different theoretical models describing the excitation process.

In the present study, the evolution of the satellite structure in the photoinduced *KLL* Auger spectra of Cu and Ni metals is studied at photon energies near threshold. For the data analysis, a realistic physical model is used by applying energy loss probabilities derived from reflection electron energy loss spectroscopy (REELS) for the correction of the experimental Cu and Ni *KLL* spectra for electron scattering within the metallic samples. This allows for an accurate separation of contributions from extrinsic and intrinsic excitations in the spectra. The experimental results reveal a clearly different behavior for particular satellites, which can be unambiguously attributed to excitations in the initial and final states, respectively. The dependence of the satellite intensities on the photon energy is compared to the prediction of Thomas model[8] and to calculations using a generic computation method to estimate the probability of initial state shake up processes.

II. EXPERIMENT

High-energy resolution $KL_{23}L_{23}$ Auger spectra of clean high-purity polycrystalline Cu and Ni foils were obtained using the tunable high-energy x-ray photoelectron spectroscopy facility at the BW2 beamline of HASYLAB.[9] The photon energy was fine tuned in the near-threshold region up to about 50 eV above the *K*-absorption edge. The photon energy bandwidth at the Cu and Ni *K* edge was 1.50 eV and 1.35 eV, respectively, while the energy resolution of the electron spectrometer was 0.2 eV. The kinetic energy scale was calibrated using the main diagram line of the Au $M_5N_{6,7}N_{6,7}$ Auger spectrum (at 2015.8 eV). The absolute electron energies are expected to be accurate within ±0.3 eV. The Auger spectra were corrected for background from inelastically scattered electrons applying Tougaard's method[10] with experimental cross sections for inelastic electron scattering. These were derived from high-energy resolution REELS spectra of the same sample, measured using the ESA-31 electron spectrometer of ATOMKI based on a hemispherical analyzer.[11] The primary electron-beam energy was chosen to match the kinetic energy of the $^1D_2$ (KL_2L_3) Auger electrons. Simultaneous evaluation of the background corrected spectra was performed by fitting the respective peaks with asymmetric Lorentzians. Here, it was assumed that the energy separation and the line shape of the components are independent of the exciting photon energy. It is noted, however, that the peaks become slightly asymmetric near threshold due to the Auger resonant Raman process. The observed satellite lines were associated with the strongest spectral line [namely to the $^1D_2$ (KL_2L_3) diagram line]. The other much less intense Auger diagram lines may also have similar (or different) satellites hidden in the background, but no experimental evidence of their existence can be seen in the spectra, therefore their contribution has been neglected during the data evaluation.

III. MODEL CALCULATIONS

A. Satellite-main peak energy separation

In the $KL_{23}L_{23}$ Auger spectra of Cu and Ni, excited using nonmonochromatic x-rays, two satellite lines are observed.[1,12,13] On the basis of the excited atom model[14,15] and atomic calculations, the satellite found at the smaller energy separation (Sat 2) from the most intense $^1D_2$ diagram line was attributed to a 3*d* spectator vacancy satellite assumed to occur due to an intraatomic 3*d* shake-up process during the 1*s* photoionization.[1,2] To estimate the energy separation ΔE_{Sat2} between the main Auger peak and the satellite, cluster molecular orbital calculations were performed[2] using the discrete variational (DV) $X\alpha$ model.[16] For Cu and Ni, the results for ΔE_{Sat2} are in good agreement with the experiment. The model also predicts the large difference of ΔE_{Sat2} between Cu and Ni attributing it to screening effects.[2]

In this work, a similar approach was followed to interpret the energy position of the other satellite (Sat 1) found at larger energy separation, assuming that it appears as a consequence of final state effects, i.e., due to a 3*d* shake-up process following the appearance of a 2*p* core hole in the final state of the $KL_{23}L_{23}$ Auger transition.

The energy position of the satellite line (Sat 1) relative to the diagram line is given by

$$\Delta E_{\mathrm{sat}} = (E_i - E_f) - (E_i - E_f') = E_f - E_f', \tag{1}$$

where E_i is the total energy of the atom or cluster in the $1s^12p^63d^n4s^m$ initial state, E_f' is the total energy in the $1s^22p^43d^n4s^m$ final state and E_f' is the total energy in the $1s^22p^43d^{n-1}4s^m$ final state in which there is an extra 3*d* vacancy due to a $3d \rightarrow 4d$ (or higher) monopole excitation.

Expression (1) was approximated by the difference of the 3*d* and 4*d* one-electron energies obtained from Slater-type transition state[16] calculations, where one-half of an electron was removed from the 3*d* state and added to the 4*d* orbital in the central atom (with the two 2*p* holes in the final state of the *KLL* Auger transition). This simple calculation scheme is very similar to that one derived by Kleiman[15] on the basis of the "excited atom" model[14] applied to Auger satellites. The main difference is that in our case the $3d \rightarrow 4d$ excitation energy is calculated in a cluster environment (modeling solid state effects), and the screening of the two core holes in the final state is taken into account by charge neutralization of the cluster instead of the "$Z+2$" approximation used in the "excited atom" model. The simple scheme derived by Kleiman *et al.*[15] is based on the assumption that the multiplet structure of the Auger spectrum is mainly determined by the interaction of the two core holes in the final state of the Auger transition, while the extra multiplet interaction caused by the spectator vacancy created in the valence band is negligible (except of a slight broadening of the satellite line). Their results obtained for the Ag *LMM* Auger spectra[15] confirmed the validity of this assumption and are likewise applicable to similar cases (such as the Cu, Ni *KLL* spectra presented here).

In these calculations performed by using the *DV-X*α model and the self-consistent charge method,[16] a simple cluster consisting of 13 atoms was adopted to model the regular face-centered-cubic lattice of the Cu and Ni metals. A near minimal base set of the atomic orbitals was applied ($1s-4d$ for the central atom and $1s-4p$ for the 12 equivalent neighboring atoms). The pairs of molecular orbitals corresponding to 3*d* and 4*d* atomic orbitals were found from Mulliken population analysis. This analysis shows that the 3*d* orbital of the central atom dominates the $8e_g$ and $8t_{2g}$ symmetry orbitals, while the 4*d* atomic orbital dominates in the orbitals $15e_g$ and $16t_{2g}$.[2] It was shown earlier[2] that such an approximation (based on a cluster of 13 atoms), completed with the charge neutralization on the cluster (to compensate for excess charge created by the ionisation and the Auger processes), led to a result comparable to that obtained for a larger cluster (43 atoms). It is therefore believed that it accounts well for solid-state effects, such as core hole screening by the conduction electrons.

B. Dependence of the satellite intensity on the exciting photon energy near threshold

1. Thomas' model

In the case of photoionization close to the threshold, the ejected photoelectron has a low velocity and the atomic po-

TABLE I. $KL_{23}L_{23}$ Auger satellite—$^1D_2$ (KL_2L_3) peak separations (eV).

	Cu		Ni	
	Sat 1	Sat 2	Sat 1	Sat 2
XAES[a]	39.0	11.9	31.7	6.4
Present work	35.7	11.4	31.3	7.3
DV-Xα results				
$8e_g \rightarrow 15e_g$	37.2	10.2[b]	30.9	5.7[b]
$8t_{2g} \rightarrow 16t_{2g}$	35.8	10.6[b]	30.4	6.4[b]

[a]See Ref. 12.
[b]See Ref. 2.

tential is slowly changes upon the appearance of the core hole. The atomic orbitals can therefore relax adiabatically and atomic excitations can be influenced by the Coulomb interaction with the ejected electron.

Such processes should be treated using a time-dependent approach—contrary to the case of highly energetic photoelectrons where the transition of the additional excited electron is caused by the *sudden* change in the atomic potential upon core hole creation. In that case, the probability of the excitation is independent of the photon energy, and usually well approximated by the overlap integral between initial and final state wave functions. Thomas solved the time-dependent Schrödinger equation approximating the change in the atomic potential due to the slowly moving photoelectron by an error function.[8] By simplifying the assumptions, the transition probability μ for an electron excited into an unoccupied state is given by $\mu=\mu_\infty \exp(-mr^2\Delta E^2/2\hbar^2 E_{ex})$, where μ_∞ is the transition probability in the sudden limit, r is

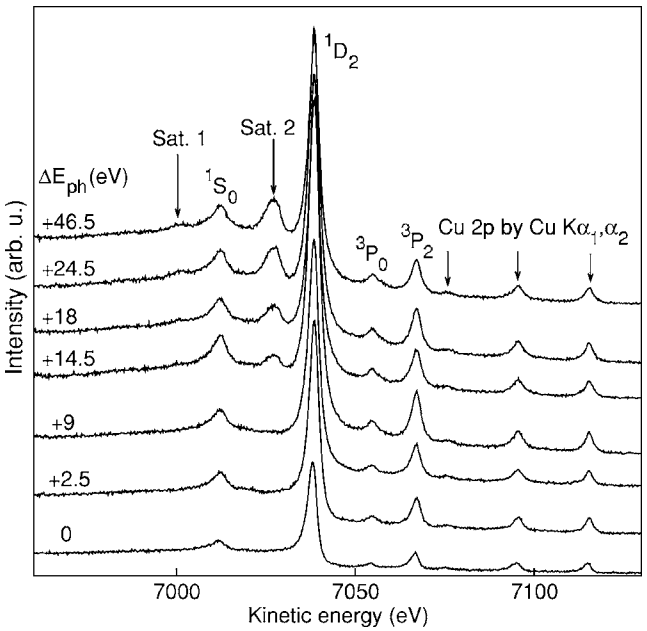

FIG. 1. Cu $KL_{23}L_{23}$ Auger spectra photoexcited from Cu metal as a function of the photon energy above threshold (ΔE). The spectra are normalized to absolute intensity (in arb. units).

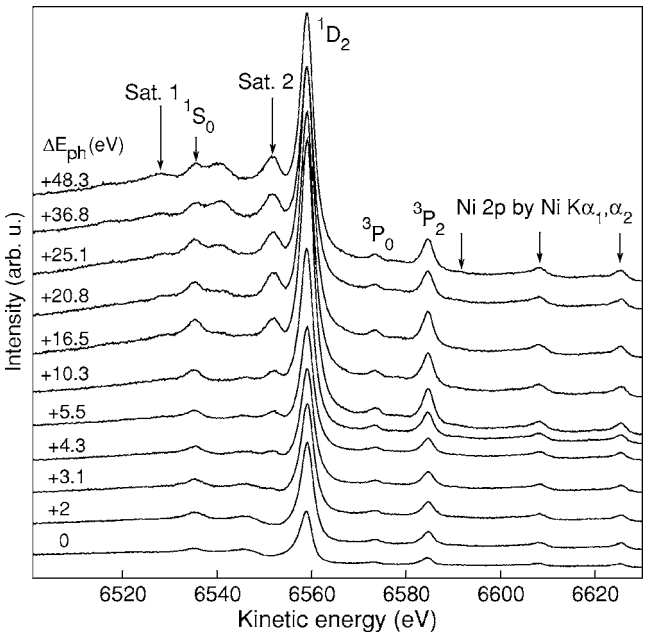

FIG. 2. Ni $KL_{23}L_{23}$ Auger spectra photoexcited from Ni metal as a function of the photon energy above threshold (ΔE). The spectra are normalized to absolute intensity (in arb. units). Additional (initial-state) satellite structure is seen between $^1S_0$ and Sat. 2, which is not discussed here. In the spectra of Ni, very close to the threshold, the broad structure around 6545 eV shows the effects of the unoccupied density of states (see Ref. 22) and possibly some contributions due to collective excitation of electrons in the metal by the appearance of the core hole(s).

the atomic dimension, ΔE is the energy transferred to the excited electron (shake-up energy), and $E_{ex}=E_{ph}-E_{th}$ is the excess photon energy above threshold (E_{ph} denotes the photon energy and E_{th} the threshold energy). $E_{th}=E_K+\Delta E$, where E_K is the binding energy of the 1*s* electrons. Our results show that by using the above definition for E_{th}, a good agreement is obtained between experiment and theory.

2. Generic computation model

For the interpretation of the measured data, theoretical calculations were carried out combining the Thomas model[8] with the Waseda model[17] for the shake-up processes induced near the *K*-absorption threshold in Cu and Ni metals with up to 50 eV excess photon energy. It was assumed that the intensity of the initial state type shake-up satellite line—relative to that of the KL_2L_3 ($^1D_2$) main line—as a function of the incident photon energy is largely proportional to the probability of the $3d \rightarrow 4d$ intrinsic excitation. The energy dependence of this multiple-electron excitation probability was determined. In the calculations (based on a free-atom description in one-electron terms), both the active and passive electron approximations were applied. The passive (unexcited) electrons were taken into account by a screened nuclear charge, and the probability for the transition of the active electron from an occupied bound state to an unoccupied bound state was calculated.

Following Thomas,[8] we approximate the perturbation potential for the core photoelectron system as a product of

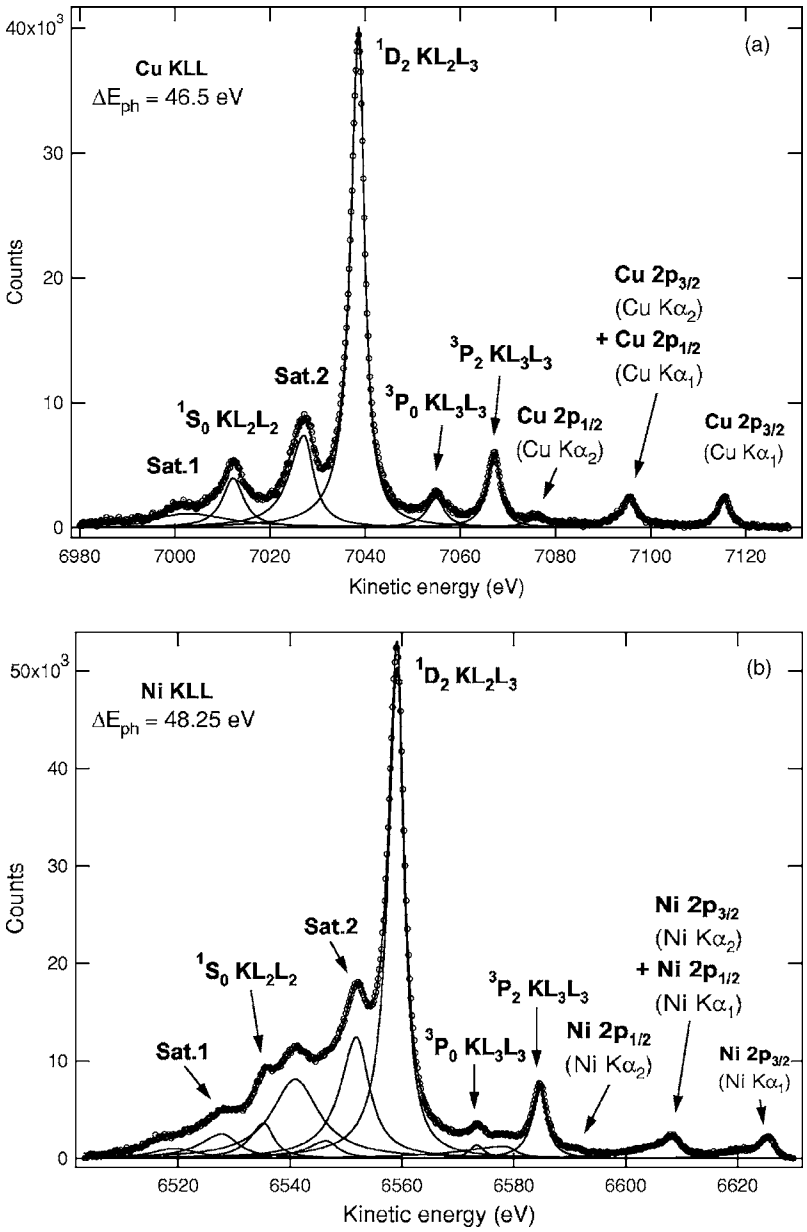

FIG. 3. Example for the evaluation of the Cu (a) and Ni (b) $KL_{23}L_{23}$ Auger spectra following corrections for background from inelastically scattered electrons.

position-dependent and time-dependent parts:

$$V(\mathbf{r},t) = V_{\mathrm{nl}}(\mathbf{r})f(t). \tag{2}$$

According to the Waseda model,[17] the change in the central potential for the jth electron due to the removal of the ith electron from a subshell can be approximated using the matrix element $V_{\mathrm{nl}}(\mathbf{r}_j) = -\langle\varphi_i(\mathbf{r}_i)|\mathbf{r}_{ji}^{-1}|\varphi_i(\mathbf{r}_i)\rangle$, in which only the monopole term remains. The $\varphi(\mathbf{r})$ wave functions are one-electron spinors belonging to the unperturbed Hamiltonian of the free atom before the ionization, $\mathbf{r}$ denotes the position vector of the electron measured from the nucleus, and $\mathbf{r}_{ji}$ is the difference between the position vectors of the respective electrons. The position-dependent potential term in Eq. (2) was calculated using single-zeta radial wave functions[18] and can be written in the form

$$V_{\mathrm{nl}}(r) = -N_{\mathrm{nl}}^2/(2\zeta_{\mathrm{nl}})^{2n}[(1/2r\zeta_{\mathrm{nl}})\gamma(2n+1,r) + \Gamma(2n,r)], \tag{3}$$

where $\gamma(k,r)$ *and* $\Gamma(k,r)$ are the incomplete gamma functions,[19] $\zeta_{\mathrm{nl}} = (Z - \sigma_{\mathrm{nl}})/n$, where Z is the nuclear charge on the atom, σ_{nl} is the screening parameter, N_{nl} is a normalization constant, and n and l are the principal and orbital quantum numbers, respectively. For the time-dependent factor, the approximate form $f(t) = 1 - \exp(-t/t_0)$, proposed by Gadzuk and Sunjic,[20] was adopted. The characteristic time t_0 can be calculated for the shaken electron using the following expression:[21]

$$t_0 = (n-1)/(\zeta_{\mathrm{nl}}\sqrt{(2(E_{\mathrm{ph}} - E_{\mathrm{th}}))}), \tag{4}$$

where E_{ph} is the energy of the incident photon and E_{th} is the threshold energy which is equal to the binding energy of the passive $1s$ electron plus the shake-up energy: $E_{\mathrm{th}} = E_K + \Delta E$

and $\Delta E = E_{3d} - E_{4d}$. These quantities can be obtained using the standard Hartree–Fock method. The probability of the transition in the first order can be expressed as:[8,17,21]

$$P^{1s}_{3d-4d}(E_{\mathrm{ph}}) = |\langle \varphi_{4d}(r)|V_{1s}(r)|\varphi_{3d}(r)\rangle|^2/(\Delta E^2[1+\Delta E^2 t_0^2]). \quad (5)$$

Using the single-zeta wave functions, the matrix element in Eq. (5) can be written in a simple analytical form. In the low-energy limit, the shake-up probability approaches zero, while in the extreme high photon energy limit (sudden approximation) the shake-up probability tends to reach an energy independent value

$$P^{1s}_{3d-4d}(E_{\mathrm{ph}} \to \infty) = |\langle \varphi_{4d}(r)|V_{1s}(r)|\varphi_{3d}(r)\rangle|^2/\Delta E^2. \quad (6)$$

IV. RESULTS AND DISCUSSION

The results of the experiment and the model calculations are presented in Table I and in Figs. 1–4. Figures 1 and 2 show measured Cu and Ni $KL_{23}L_{23}$ Auger spectra as a function of the excess photon energy above the metal K edges. The K-absorption spectra were measured by recording the total electron yield (drain current from the sample). The threshold position was defined as the inflection point of the leading absorption edge structure. For Cu (Fig. 1), two types of satellites can be identified in the spectra. The intensity of the first type (Sat. 2, which is the most intense for off-resonant excitation) quickly decreases when the photon energy is lowered toward the ionization threshold. The intensity of the second type (Sat. 1) changes more slowly as revealed by the detailed analysis of the spectra (Fig. 4). The spectra of Ni (Fig. 2) show the corresponding satellites but also an additional structure (between $^1S_0$ and Sat. 2) mainly of initial state type, which exhibits a pronounced intensity modulation near threshold. The overall picture is more complicated compared to Cu owing to additional correlational interactions with the partially open $3d$ shell and this satellite will not be discussed here.

Due to the high-energy resolution and photon flux in this experiment the ^3P lines at the high kinetic energy side of $^1D_2$ are nicely resolved in the spectra. In addition, the $2p$ photoelectrons excited by $K\alpha$ fluorescence *internally* within the thick samples, are observed as well. Approaching the K-shell threshold, the peaks become slightly asymmetric which is a fingerprint of the Auger resonant Raman process.[22,23] In Fig. 3, typical fit results of the Cu and Ni $KL_{23}L_{23}$ Auger spectra are shown, which have been corrected for the background from inelastically scattered electrons. In the case of Ni, at photon energies far from the threshold, a wide pronounced additional structure near 6540 eV kinetic energy can be seen which disappears at near threshold excitation, indicating that it can be attributed to initial state excitations. This structure was barely visible in previous work.[13]

The energy separations of the satellites from the $^1D_2$ (KL_2L_3) main Auger peak $\Delta E_{\mathrm{Sat}} = E(^1D_2) - E(\mathrm{Sat})$ are summarized in Table I. They are compared with values obtained from the respective DV-$X\alpha$ cluster molecular orbital calculations. The values for ΔE_{Sat} in Table I show a good agreement between the experiment and the model calculations both for Cu and Ni, i.e., the experimental data confirm the assumptions of the models concerning the origin of Sat 1 (final state type) and Sat 2 (initial state type). Also, both experiment and model calculations yield considerable smaller values of ΔE_{Sat} for Ni compared to Cu, which is due to the difference in screening.[2] Direct additional information on the character of the satellites is obtained from the variation of their intensity as a function of the excess photon energy, the "evolution curve," which is in general expected to be quite different for initial and final state type satellites. By lowering the photon energy toward threshold excitation, the intensity of the initial state type satellite should drop rapidly at excess energies lower than the required shake-up energy. In the case of a final state type satellite, its intensity is not expected to depend on the excess photon energy above threshold. Therefore, the measured satellite intensity behavior yields direct information on the nature of the particular

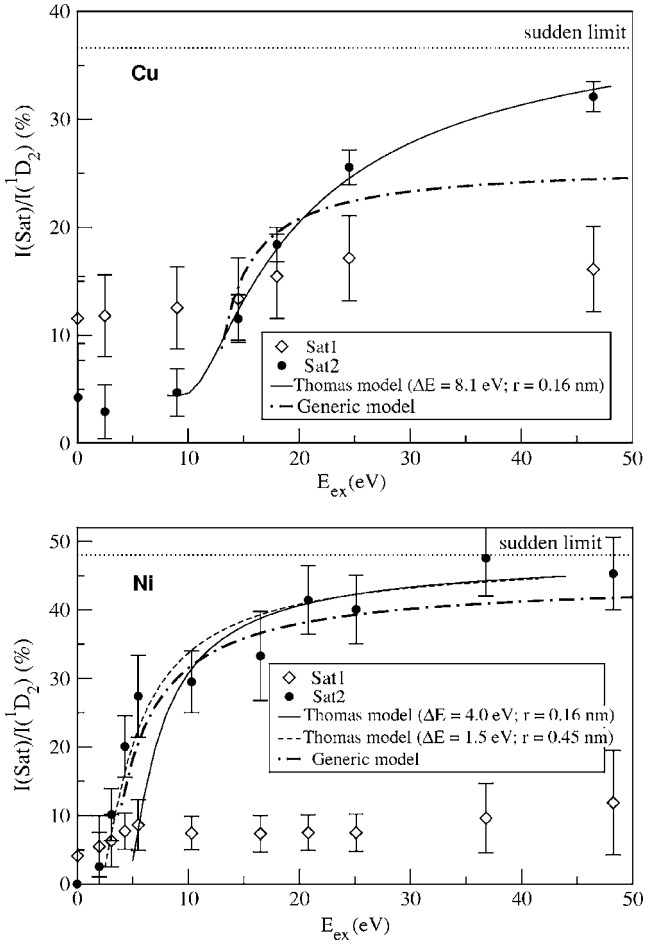

FIG. 4. Evolution of the Cu and Ni $KL_{23}L_{23}$ Auger satellite intensities relative to the $^1D_2$ main line (Sat 1: "Final state shake-up;" Sat 2: "initial state shake-up") as a function of excess photon energy E_{ex} above the K-shell ionization threshold. The satellite intensity is shown *relative* to the intensity of the $^1D_2$ diagram line (following background correction and peak fitting of the spectra, as shown in Fig. 3). Theoretical predictions for the Sat 2 intensities obtained by the Thomas (Ref. 8) and the generic models are also shown for comparison.

excitation which is consistent with the calculated ΔE_{Sat} within the assumed model. The intensity data for Sat 1 and Sat 2 for both Cu and Ni (Fig. 4) confirm this consistency, indeed, indicating that the Sat 2 satellites are excited during the creation of the initial $(1s)$ core hole, while the Sat 1 satellites are induced in the process of the appearance of the final state core holes of the Auger transition. In Fig. 4, theoretical predictions for the Sat 2 intensities obtained by the Thomas and the generic computation models are also shown for comparison. Specifically, in the case of Ni, the general agreement between experiment and theory is quite satisfactory, the parameters used in the Thomas model have reasonable values. The generic model gives a similar tendency as the Thomas model and the experiment, however, it suggests a somewhat lower value for the sudden limit. For Cu, the experimental data are in a good agreement with the prediction of the Thomas formula, using realistic values for the model parameters. The generic model predicts, in general, a similar satellite intensity variation, although it suggests a considerably lower value for the sudden limit, which is not confirmed by the experiment.

V. CONCLUSIONS

The evolution of $KL_{23}L_{23}$ Auger satellite structures, photoexcited near threshold from Cu and Ni metals, was measured as a function of photon energy and compared to predictions of simple theoretical models. The energy separations between the satellites and the $^1D_2$ main diagram Auger line were obtained from the experimental spectra and interpreted using a cluster molecular orbital model. The results presented in Table I and in Figs. 1–4 show that both "initial state" and "final state" type satellites are present in the spectra of both Cu and Ni. The respective evolution curves of the satellite intensities, as well as the satellite-main Auger line energy separations ΔE_{Sat}, can be consistently interpreted by theoretical models based on atomic and cluster molecular orbital calculations confirming that the satellite found at small ΔE_{Sat} can be attributed to an initial state $3d \rightarrow 4d$ shake excitation, while the satellite found at larger ΔE_{Sat} is due to a shake-up excitation in the final state.

ACKNOWLEDGMENTS

The financial support of Grant No. OTKA T038016 and JSPS-MTA No. 59 is acknowledged. This work was supported by the European Union—Research Infrastructure Action under the FP6 "*Structuring the European Research Area*" Programme (through the Integrated Infrastructure Initiative "*Integrating Activity on Synchrotron and Free Electron Laser Science*").

[1] L. Kövér, Zs. Kovács, J. Tóth, I. Cserny, D. Varga, P. Weightman, and S. Thurgate, Surf. Sci. **433**, 833 (1999).
[2] I. Cserny, L. Kövér, H. Nakamatsu, and T. Mukoyama, Surf. Interface Anal. **30**, 199 (2000).
[3] D. D. Sarma, C. Carbone, P. Sen, R. Cimino, and W. Gudat, Phys. Rev. Lett. **63**, 656 (1989).
[4] G. Curró, R. Cosso, M. Sancrotti, L. Duó, S. D'Addato, S. Nannarone, S. Iacobucci, G. Panaccione, and P. Weightman, Phys. Rev. B **46**, 15652 (1992).
[5] D. D. Sarma, S. R. Barman, R. Cimino, C. Carbone, P. Sen, A. Roy, A. Chainani, and W. Gudat, Phys. Rev. B **48**, 6822 (1993).
[6] M. Magnuson, N. Wassdahl, A. Nilsson, A. Föhlisch, J. Nordgren, and N. Mårtensson, Phys. Rev. B **58**, 3677 (1998).
[7] W. Drube, T. M. Grehk, R. Treusch, G. Materlik, J. E. Hansen, and T. Åberg, Phys. Rev. B **60**, 15507 (1999); and further references therein.
[8] T. D. Thomas, Phys. Rev. Lett. **52**, 417 (1984).
[9] W. Drube, T. M. Grehk, R. Treusch, and G. Materlik, J. Electron Spectrosc. Relat. Phenom. **88**, 683 (1998).
[10] S. Tougaard, Surf. Interface Anal. **26**, 249 (1998).
[11] L. Kövér, D. Varga, I. Cserny, J. Tóth, and K. Tőkési, Surf. Interface Anal. **19**, 9 (1992).
[12] L. Kövér, D. Varga, I. Cserny, J. Tóth, and Zs. Kovács, J. Surf. Anal. **5**, 74 (1999).
[13] L. Kövér, I. Cserny, J. Tóth, D. Varga, and T. Mukoyama, J. Electron Spectrosc. Relat. Phenom. **114**, 55 (2001).
[14] A. R. Williams and N. D. Lang, Phys. Rev. Lett. **40**, 954 (1978).
[15] G. G. Kleiman, S. G. C. de Castro, and R. Landers, Phys. Rev. B **49**, 2753 (1994).
[16] H. Adachi, M. Tsukada, and C. Satoko, J. Phys. Soc. Jpn. **45**, 875 (1978).
[17] T. Mukoyama and M. Uda, Phys. Rev. A **61**, 030501(R) (2000).
[18] E. Clementi and C. Roetti, At. Data Nucl. Data Tables **14**, 177 (1974).
[19] M. Abramowitz and I. A. Stegun, *Handbook of Mathematical Functions*, Natl. Bur. Stand. (U.S.A.) Applied Mathematics Series, Vol. 55 (U.S. GPO, Washington D.C., 1964), integral formula 6.5.1–3, p. 260, and formula 6.5.13, p. 262.
[20] J. W. Gadzuk and M. Sunjic, Phys. Rev. B **12**, 524 (1975).
[21] M. Roy, J. D. Lindsay, S. Louch, and S. J. Gorman, J. Synchrotron Radiat. **8**, 1103 (2001).
[22] W. Drube, R. Treusch, and G. Materlik, Phys. Rev. Lett. **74**, 42 (1995).
[23] T. Åberg, Phys. Scr., T **41**, 71 (1992).